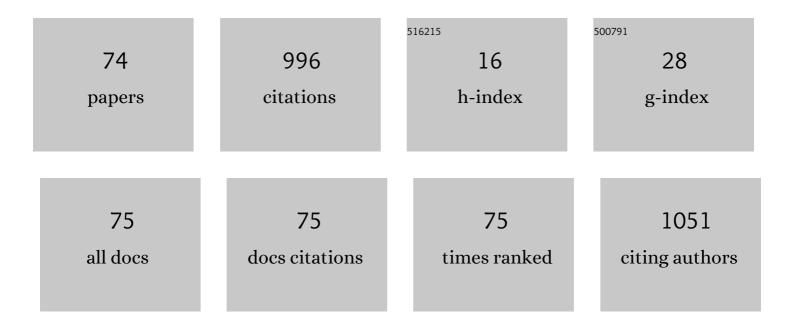
List of Publications by Year in descending order

Source: https://exaly.com/author-pdf/7267020/publications.pdf Version: 2024-02-01



FRANCA LINNATTA

#	Article	IF	CITATIONS
1	Prostate Segmentation: An Efficient Convex Optimization Approach With Axial Symmetry Using 3-D TRUS and MR Images. IEEE Transactions on Medical Imaging, 2014, 33, 947-960.	5.4	64
2	Three-dimensional ultrasound of carotid atherosclerosis: Semiautomated segmentation using a level set-based method. Medical Physics, 2011, 38, 2479-2493.	1.6	60
3	Interactive Hierarchical-Flow Segmentation of Scar Tissue From Late-Enhancement Cardiac MR Images. IEEE Transactions on Medical Imaging, 2014, 33, 159-172.	5.4	57
4	Dual optimization based prostate zonal segmentation in 3D MR images. Medical Image Analysis, 2014, 18, 660-673.	7.0	46
5	Convolutional neural networkâ€based approach for segmentation of left ventricle myocardial scar from 3D late gadolinium enhancement <scp>MR</scp> images. Medical Physics, 2019, 46, 1740-1751.	1.6	44
6	Automated classification of solid renal masses on contrast-enhanced computed tomography images using convolutional neural network with decision fusion. European Radiology, 2020, 30, 5183-5190.	2.3	43
7	Myocardial Infarct Segmentation From Magnetic Resonance Images for Personalized Modeling of Cardiac Electrophysiology. IEEE Transactions on Medical Imaging, 2016, 35, 1408-1419.	5.4	41
8	A Voxel-Based Fully Convolution Network and Continuous Max-Flow for Carotid Vessel-Wall-Volume Segmentation From 3D Ultrasound Images. IEEE Transactions on Medical Imaging, 2020, 39, 2844-2855.	5.4	40
9	3-D Carotid Multi-Region MRI Segmentation by Globally Optimal Evolution of Coupled Surfaces. IEEE Transactions on Medical Imaging, 2013, 32, 770-785.	5.4	39
10	Imageâ€based reconstruction of threeâ€dimensional myocardial infarct geometry for patientâ€specific modeling of cardiac electrophysiology. Medical Physics, 2015, 42, 4579-4590.	1.6	38
11	Automated segmentation of prostate zonal anatomy on T2â€weighted (T2W) and apparent diffusion coefficient (<scp>ADC</scp>) map <scp>MR</scp> images using Uâ€Nets. Medical Physics, 2019, 46, 3078-3090.	1.6	36
12	Threeâ€dimensional segmentation of threeâ€dimensional ultrasound carotid atherosclerosis using sparse field level sets. Medical Physics, 2013, 40, 052903.	1.6	33
13	Fully automated segmentation of left ventricular scar from 3D late gadolinium enhancement magnetic resonance imaging using a cascaded multiâ€planar Uâ€Net (CMPUâ€Net). Medical Physics, 2020, 47, 1645-1655.	1.6	32
14	Threeâ€dimensional prostate segmentation using level set with shape constraint based on rotational slices for 3D endâ€firing TRUS guided biopsy. Medical Physics, 2013, 40, 072903.	1.6	25
15	Fast interactive multi-region cardiac segmentation with linearly ordered labels. , 2012, , .		21
16	Quantification and visualization of carotid segmentation accuracy and precision using a 2D standardized carotid map. Physics in Medicine and Biology, 2013, 58, 3671-3703.	1.6	21
17	Rotational-Slice-Based Prostate Segmentation Using Level Set with Shape Constraint for 3D End-Firing TRUS Guided Biopsy. Lecture Notes in Computer Science, 2012, 15, 537-544.	1.0	19
18	Detection of COVID-19 from chest x-ray images using transfer learning. Journal of Medical Imaging, 2021, 8, 017503.	0.8	18

#	Article	IF	CITATIONS
19	Sensitive threeâ€dimensional ultrasound assessment of carotid atherosclerosis by weighted average of local vessel wall and plaque thickness change. Medical Physics, 2017, 44, 5280-5292.	1.6	15
20	Myocardial scar segmentation from magnetic resonance images using convolutional neural network. , 2018, , .		14
21	Rotationally resliced 3D prostate TRUS segmentation using convex optimization with shape priors. Medical Physics, 2015, 42, 877-891.	1.6	13
22	Automated segmentation of villi in histopathology images of placenta. Computers in Biology and Medicine, 2019, 113, 103420.	3.9	13
23	Cascaded Triplanar Autoencoder M-Net for Fully Automatic Segmentation of Left Ventricle Myocardial Scar From Three-Dimensional Late Gadolinium-Enhanced MR Images. IEEE Journal of Biomedical and Health Informatics, 2022, 26, 2582-2593.	3.9	13
24	Fully automated segmentation of left ventricular myocardium from 3D late gadolinium enhancement magnetic resonance images using a U-net convolutional neural network-based model. , 2019, , .		12
25	Coupled level set approach to segment carotid arteries from 3D ultrasound images. , 2011, , .		11
26	Evaluation of fully automated myocardial segmentation techniques in native and contrastâ€enhanced T1â€mapping cardiovascular magnetic resonance images using fully convolutional neural networks. Medical Physics, 2021, 48, 215-226.	1.6	11
27	Fully automated localization of prostate peripheral zone tumors on apparent diffusion coefficient map MR images using an ensemble learning method. Journal of Magnetic Resonance Imaging, 2020, 51, 1223-1234.	1.9	10
28	Machine vision system for automated spectroscopy. Machine Vision and Applications, 2012, 23, 111-121.	1.7	9
29	Efficient 3D Endfiring TRUS Prostate Segmentation with Globally Optimized Rotational Symmetry. , 2013, , .		9
30	A Fast Convex Optimization Approach to Segmenting 3D Scar Tissue from Delayed-Enhancement Cardiac MR Images. Lecture Notes in Computer Science, 2012, 15, 659-666.	1.0	9
31	Efficient 3D Multi-region Prostate MRI Segmentation Using Dual Optimization. Lecture Notes in Computer Science, 2013, 23, 304-315.	1.0	9
32	Three-dimensional semi-automated segmentation of carotid atherosclerosis from three-dimensional ultrasound images. Proceedings of SPIE, 2012, , .	0.8	8
33	Semi-automated segmentation of carotid artery total plaque volume from three dimensional ultrasound carotid imaging. Proceedings of SPIE, 2012, , .	0.8	8
34	Joint segmentation of lumen and outer wall from femoral artery MR images: Towards 3D imaging measurements of peripheral arterial disease. Medical Image Analysis, 2015, 26, 120-132.	7.0	8
35	Segmentation of Integrated Circuit Layouts from Scan Electron Microscopy Images. , 2018, , .		8
36	Machine Learning-Based Segmentation of Left Ventricular Myocardial Fibrosis from Magnetic Resonance Imaging. Current Cardiology Reports, 2020, 22, 65.	1.3	8

#	Article	IF	CITATIONS
37	Evaluation of Finger Flexion Classification at Reduced Lateral Spatial Resolutions of Ultrasound. IEEE Access, 2021, 9, 24105-24118.	2.6	8
38	Myocardial Infarct Segmentation and Reconstruction from 2D Late-Gadolinium Enhanced Magnetic Resonance Images. Lecture Notes in Computer Science, 2014, 17, 554-561.	1.0	8
39	Lateral Ventricle Segmentation of 3D Pre-term Neonates US Using Convex Optimization. Lecture Notes in Computer Science, 2013, 16, 559-566.	1.0	8
40	Fast Globally Optimal Segmentation of 3D Prostate MRI with Axial Symmetry Prior. Lecture Notes in Computer Science, 2013, 16, 198-205.	1.0	8
41	Image-based reconstruction of 3D myocardial infarct geometry for patient specific applications. Proceedings of SPIE, 2015, 9413, .	0.8	7
42	Fully automated detection of prostate transition zone tumors on T2â€weighted and apparent diffusion coefficient (ADC) map MR images using Uâ€Net ensemble. Medical Physics, 2021, 48, 6889-6900.	1.6	7
43	Vision Based Metal Spectral Analysis Using Multi-label Classification. , 2009, , .		6
44	Virtual electrophysiological study as a tool for evaluating efficacy of MRI techniques in predicting adverse arrhythmic events in ischemic patients. Physics in Medicine and Biology, 2018, 63, 225008.	1.6	6
45	Automated 3D Uâ€net based segmentation of neonatal cerebral ventricles from 3D ultrasound images. Medical Physics, 2022, 49, 1034-1046.	1.6	6
46	Effect of T1-mapping technique and diminished image resolution on quantification of infarct mass and its ability in predicting appropriate ICD therapy. Medical Physics, 2018, 45, 1577-1585.	1.6	5
47	Left atrial imaging and registration of fibrosis with conduction voltages using LGE-MRI and electroanatomical mapping. Computers in Biology and Medicine, 2019, 111, 103341.	3.9	5
48	Jointly Segmenting Prostate Zones in 3D MRIs by Globally Optimized Coupled Level-Sets. Lecture Notes in Computer Science, 2013, , 12-25.	1.0	5
49	Three-dimensional Ultrasound Imaging of Carotid Atherosclerosis. , 2011, , .		4
50	Segmentation of the lumen and media-adventitia boundaries of the common carotid artery from 3D ultrasound images. Proceedings of SPIE, 2011, , .	0.8	4
51	Prostate segmentation in 3D TRUS using convex optimization with shape constraint. , 2013, , .		4
52	Efficient convex optimization-based curvature dependent contour evolution approach for medical image segmentation. , 2013, , .		4
53	3D Prostate TRUS Segmentation Using Globally Optimized Volume-Preserving Prior. Lecture Notes in Computer Science, 2014, 17, 796-803.	1.0	4
54	Efficient Global Optimization Based 3D Carotid AB-LIB MRI Segmentation by Simultaneously Evolving Coupled Surfaces. Lecture Notes in Computer Science, 2012, 15, 377-384.	1.0	4

#	Article	IF	CITATIONS
55	Automatic Placental Distal Villous Hypoplasia Scoring using a Deep Convolutional Neural Network Regression Model. , 2022, , .		4
56	Fully automated estimation of the mean linear intercept in histopathology images of mouse lung tissue. Journal of Medical Imaging, 2021, 8, 027501.	0.8	3
57	3D scar segmentation from LGE-MRI using a continuous max-flow method. , 2018, , .		3
58	Vision Based Spectroscopy Simulation. , 2008, , .		2
59	Patch-Based Convolutional Neural Network for Differentiation of Cyst From Solid Renal Mass on Contrast-Enhanced Computed Tomography Images. IEEE Access, 2020, 8, 8595-8602.	2.6	2
60	Reducing Motion Impact on Video Magnification Using Wavelet Transform and Principal Component Analysis for Heart Rate Estimation. , 2021, , .		2
61	Joint Segmentation of 3D Femoral Lumen and Outer Wall Surfaces from MR Images. Lecture Notes in Computer Science, 2013, 16, 534-541.	1.0	2
62	Comparison of myocardial scar geometries generated from 2D and 3D LGE MRI. , 2018, , .		2
63	Transfer learning-based approach for automated kidney segmentation on multiparametric MRI sequences. Journal of Medical Imaging, 2022, 9, .	0.8	2
64	Semi-automatic segmentation of preterm neonate ventricle system from 3D ultrasound images. , 2014, ,		1
65	Evaluation of a T1 mapping technique for stratifying patient risk: A preliminary study using computer simulations of cardiac electrophysiology. , 2016, , .		1
66	Sci-Fri AM: Imaging - 07: Semi-Automated Segmentation of Carotid Artery Lumen and Wall from Three-Dimensional Ultrasound Images Using Level Sets. Medical Physics, 2010, 37, 3903-3903.	1.6	1
67	Automatic 3D US Brain Ventricle Segmentation in Pre-Term Neonates Using Multi-phase Geodesic Level-Sets with Shape Prior. Lecture Notes in Computer Science, 2015, , 89-96.	1.0	1
68	Longitudinal Analysis of Pre-term Neonatal Brain Ventricle in Ultrasound Images Based on Convex Optimization. Lecture Notes in Computer Science, 2015, , 476-483.	1.0	1
69	Assessment of left atrial fibrosis progression in canines following rapid ventricular pacing using 3D late gadolinium enhanced CMR images. PLoS ONE, 2022, 17, e0269592.	1.1	1
70	Distribution of guidance models for cardiac resynchronization therapy in the setting of multi-center clinical trials. , 2014, , .		0
71	Flexible and Wearable Ultrasonic Sensors and Method for Classifying Individual Finger Flexions. , 2020, , .		0
72	MO-D-220-07: Semi-Automated Segmentation Method to Quantify Carotid Atherosclerosis from 3D Ultrasound Images. Medical Physics, 2011, 38, 3718-3718.	1.6	0

#	Article	IF	CITATIONS
73	Segmentation of the Carotid Arteries from 3D Ultrasound Images. , 2014, , 131-157.		Ο
74	Cerebral Ventricle Segmentation from 3D Pre-term IVH Neonate MR Images Using Atlas-Based Convex Optimization. Lecture Notes in Computer Science, 2014, , 46-54.	1.0	0